

## Lattice strain driven dielectric insulation response of $\text{Sr}_{1-x}\text{Ca}_x\text{Bi}_2\text{Nb}_2\text{O}_9$ ceramics

Vaibhav Shrivastava

Department of Physics, Shiv Nadar University  
Gautam Buddha Nagar 203207, Uttar Pradesh, India  
vaibhav.shrivastava@snu.edu.in

Received 20 January 2016; Revised 14 May 2016; Accepted 6 July 2016; Published 8 August 2016

In this paper, effects of lattice strain on dielectric properties of  $\text{Sr}_{1-x}\text{Ca}_x\text{Bi}_2\text{Nb}_2\text{O}_9$  ( $x = 0.0-0.5$  in steps of 0.1) ceramics are reported. High frequency dipolar polarization is observed to increase for 10% calcium addition and suppresses thereafter on higher calcium concentrations. The dielectric loss values for all doped samples were lower compared to undoped one at frequencies beyond 1 kHz. The sample with  $x = 0.1$  shows room temperature dielectric constant in the range  $(130 \pm 12)$  over a wide frequency range from 50 Hz to 1 MHz also minimum dielectric loss among all other sample for the same frequency range. Remarkable increase in Curie temperature ( $T_c$ ) by  $50^\circ\text{C}$  is recorded in the present work by increasing 10% calcium content in SBN composition. All higher doped samples indicate increase in  $T_c$  by further higher amount. In addition, dc conductivity of all samples is measured for all samples and increase in calcium content is observed to generate more insulating compositions compared to undoped SBN with higher intrinsic activation energies.

**Keywords:** Lattice strain; microstructure; dielectric constant; dielectric loss; dc conductivity.

### 1. Introduction

Aurivillius ceramics have drawn attention due to fatigue endurance and high Curie temperature.<sup>1</sup> For NvRAM applications and for use as dielectric in capacitors, lead-based ceramics like PZT, PMN-PT are popular.<sup>2</sup> Bismuth layer ceramics have advantage over lead-based zirconia ceramics as the latter undergo degradation in storage properties after about  $10^6$  cycles as against  $10^{12}$  cycles for bismuth layer ceramics.<sup>3</sup> Among bismuth layer ceramics,  $\text{SrBi}_2\text{Nb}_2\text{O}_9$  (SBN) and  $\text{SrBi}_2\text{Ta}_2\text{O}_9$  (SBT) are important because of their less distorted octahedral structure and because of sufficient influence of rattling space on the dielectric and ferroelectric properties of these materials.<sup>4</sup> These ceramics show high value of Curie temperature and fatigue resistance, but suffer from high dielectric loss and low dielectric constant for which presence of space charges in the structure is believed to be the cause.<sup>5</sup> The space charge is normally produced because of structural losses during sample preparation or due to off-valent additives or both.<sup>6</sup> In a few reports published earlier,<sup>7</sup> 10 atomic % doping of calcium in SBN system has been reported to yield an increase in Curie temperature and lowering of dielectric losses. In this paper, effects of calcium doping on Sr-sites in SBN ceramics on various electrical and structural properties like dielectric constant, dielectric loss as a function of frequency and temperature, dc conductivity, X-ray diffraction studies and pellet cross-section morphology variations are also reported.

### 2. Experimental

Samples were prepared using solid-state reaction method taking  $\text{SrCO}_3$ ,  $\text{CaCO}_3$ ,  $\text{Bi}_2\text{O}_3$  and  $\text{Nb}_2\text{O}_5$  (all from Aldrich) in stoichiometric proportions. The powders were thoroughly mixed and passed through sieve. Mixtures were calcined at  $900^\circ\text{C}$  in air for 2 h. Powdered samples were mixed in 2 weight-percent solution of polyvinylalcohol (Sigma-Aldrich) proportions then molded into disc shape pellets by applying pressure of 270 MPa. Pellets were sintered in air at  $1150^\circ\text{C}$  for 2 h. Relative density for all the pellets was measured using gravity bottle method. X-ray diffractograms of all calcined and sintered samples were taken in range  $10^\circ \leq 2\theta \leq 70^\circ$  at a scanning rate of  $0.05^\circ/\text{s}$  on a Philips X-ray diffractometer PW3710 using  $\text{CuK}\alpha$  radiation of wavelength  $1.54439 \text{ \AA}$ . Scanning electron microscope (SEM) photographs were recorded using Cambridge Stereo Scan 360 instrument. All pellets were coated using silver paste and cured at  $600^\circ\text{C}$  for half an hour. Dielectric measurements were taken on an HP 4192A Impedance Analyzer operating at an oscillation level of 1 V in the frequency range 50 Hz–1 MHz. The Curie temperature measurements were taken at a frequency of 100 kHz. dc conductivity ( $\sigma_{dc}$ ) of all samples was measured using Keithley 617 electrometer based on conventional two-probe setup. All instantaneous resistance values were recorded on falling sample temperature at the rate of  $2^\circ\text{C}$  per min after an increase up to  $600^\circ\text{C}$ . The activation energy ( $E_a$ ) for all samples was calculated using Arrhenius equation by

calculating slope of  $\ln \sigma_{dc}$  versus temperature curves in high temperature range from 400°C to 600°C. The dielectric constant and loss values were recorded at a heating rate of 3°C per min.

### 3. Results and Discussion

Peak intensities from obtained X-ray diffractograms of all samples are shown in Fig. 1. Position of peaks indicates the formation of desired perovskite structure in all samples. The samples show similar intensity ratios and an irregular shift in position of peaks for doped samples. Although all doped samples indicate an expected shift towards lower  $d$ -values on increasing calcium content in undoped sample, however, systematic change in lattice parameters is not expected based on observed  $d$ -value shift. High crystallinity is observed in all the samples. The intensity of X-ray peaks shows an increase up to 50% in going for  $x = 0.0$ – $0.1$  and a subsequent decrease from  $x = 0.2$  to  $0.4$  samples. A small increase in intensity is again observed for  $x = 0.5$ . The intensities of peaks represent phase concentration<sup>8</sup> therefore possibly  $x = 0.1$  substitution of calcium modified perovskite phase to the maximum after this substitution phase is distorted

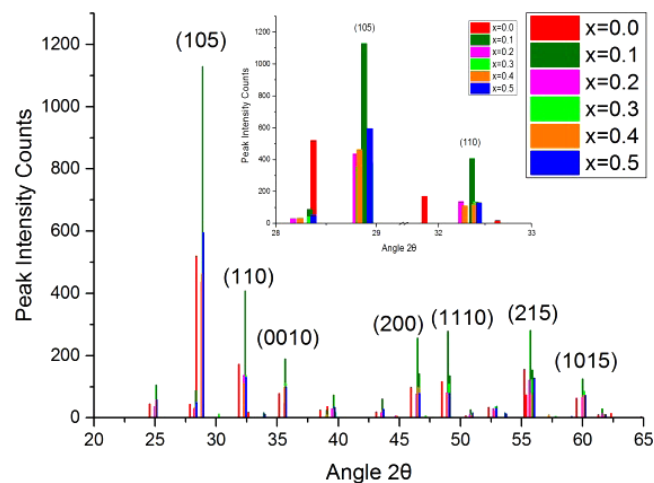


Fig. 1. X-ray diffractograms of undoped SBN and calcium doped samples (inset shows a few peak shifts).

Table 1. Lattice parameters and relative volume density with composition ( $x$ ) in  $\text{Sr}_{1-x}\text{Ca}_x\text{Bi}_2\text{Nb}_2\text{O}_9$  ceramics.

$x$	$a$ (Å)	$c$ (Å)	Relative density (in %)
0.0	3.94	25.42	92
0.1	3.90	25.19	97
0.2	3.91	25.26	97
0.3	3.91	25.28	98
0.4	3.92	25.37	99
0.5	3.91	25.33	99

Table 2. Elements in most stable valence state with their ionic radius (IR), coordination number (CN) and bond energy with oxygen.<sup>14</sup>

	IR (Å)	CN	Bond energy (kJ/mole)
$\text{Sr}^{2+}$	1.44	12	426
$\text{Ca}^{2+}$	1.34	12	403
$\text{Bi}^{3+}$	0.96	5	336
$\text{Nb}^{5+}$	0.64	6	703

comparatively. All diffraction peaks are indexed in tetragonal space group  $I4/mmm$ , popularly known<sup>9</sup> for lattice parameters calculations in these ceramics. Lattice parameters are calculated using observed  $d$ -values from diffractograms and listed in Table 1.

For these calculations, intensity peaks (200) and (0010) are chosen. The substitution of calcium onto the sites of strontium is studied on the basis of ionic radius and coordination number as listed in Table 2. The substitution of smaller calcium on the sites of strontium should reduce rattling space. This compression should result in a decrease in lattice parameters however; changes in lattice parameters with increase in calcium content are insignificant. Such a little variation in lattice parameters with composition has also been observed by others.<sup>10</sup> Moret *et al.*<sup>11</sup> reported that these Aurivillius ceramic coexist in orthorhombic and tetragonal phase and this coexistence possibly allows<sup>12</sup> the indexing of X-ray peaks either in orthorhombic or in tetragonal system based on intensity ratios. The tetragonal strain ( $c/a$ ) values are shown in Fig. 2 for all samples. The observed variations in strain parameter receive support from neutron diffraction work reported by Shimakawa *et al.*<sup>13</sup> According to Shimakawa *et al.* as the size of A-site cation decreases, lattice mismatch between  $\text{TaO}_2$  and  $\text{SrO}$  planes is increased to result in higher structural distortions hence strain values.

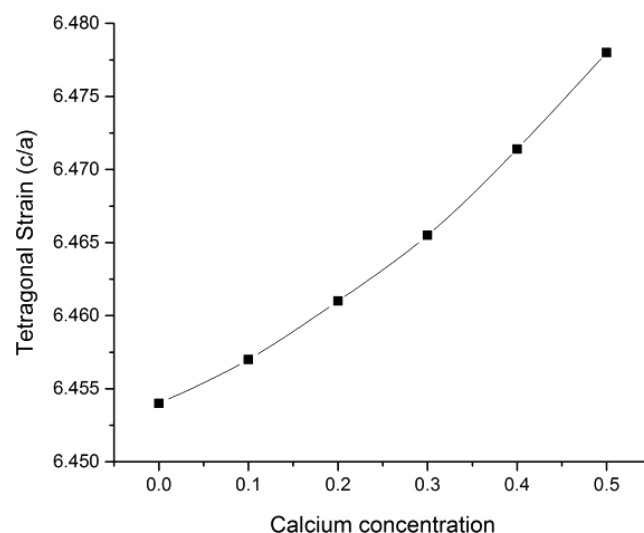


Fig. 2. Tetragonal strain values for the calcium doped samples.

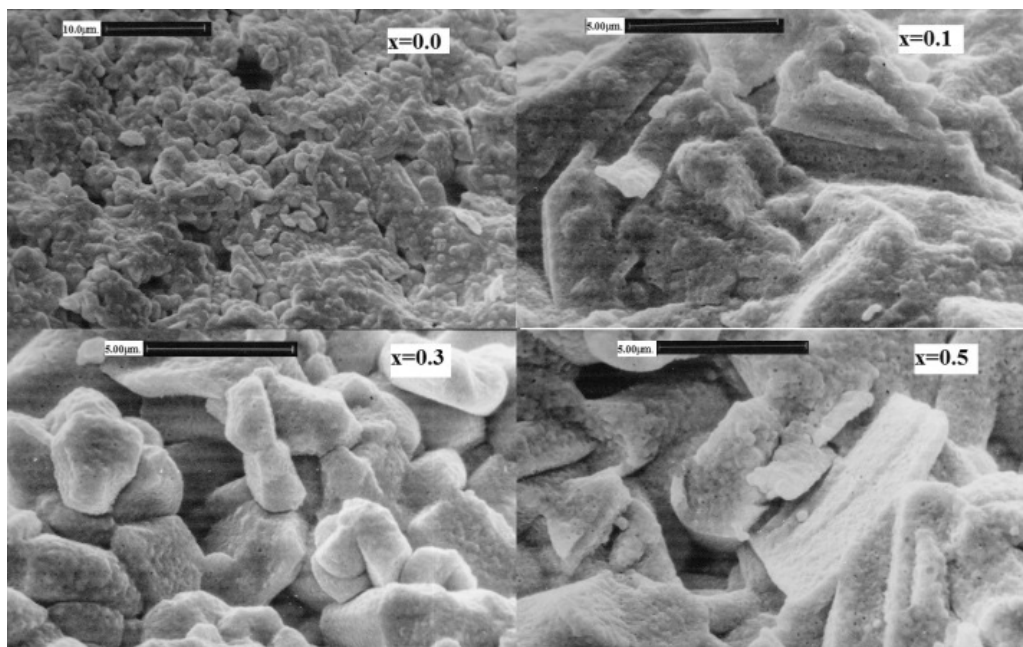


Fig. 3. SEM photographs of fracture surfaces of  $x = 0.0, 0.1, 0.3$  and  $0.5$  samples.

Figure 3 shows pellet cross-section photographs of  $x = 0.0, 0.1, 0.3$  and  $0.5$  samples. The undoped SBN sample consists of coarse grains each of average size  $7 \mu\text{m}$ . In addition, some porosity is also observed. The doping of calcium is observed to reduce porosity in doped SBN structure remarkably and induce formation of crack free microstructure. The average grain size decreases in range  $4\text{--}5 \mu\text{m}$  for calcium doped samples. All doped samples show plate shape grains with good connectivity. The doping of calcium is reported to produce plate shape grains,<sup>15</sup> which should result in low dielectric loss and leakage current in the samples. The observed morphology receives support from the measured relative density of the samples, reported in Table 1. The free charge, if any, in insulating ceramics cascades with atomic dipoles and has tendency to localize itself near electrodes, thus behaves as bound charge.<sup>16,17</sup> Such cascaded bound charge is called space charge. Therefore, the samples with microstructure similar to that of  $x = 0.1$  should show low dielectric loss and minimum space charge content. Similarly, curved grain boundaries as seen in microstructure of  $x = 0.3$  sample indicate high space charge content and low activation needed to drive dc conduction. The space charge content can be studied in samples through the slope of dielectric constant versus frequency measurements.

Figure 4 shows the variation of dielectric constant ( $\epsilon$ ) values with frequency. A slow decrease in  $\epsilon$  values is observed over the frequency range with calcium doping for  $x = 0.1$  only. Other doped samples along with undoped sample show steep decrease up to  $1 \text{ kHz}$  and a slow decrease at higher frequencies. The  $\epsilon$  values for  $x = 0.4$  and  $0.5$  is lower as compared to those of  $x = 0.2$  and  $0.3$  samples at

frequencies higher than  $5 \text{ kHz}$ . The value of  $\epsilon$  observed in present work for  $x = 0.1$  sample is greater than that reported by Forbess *et al.*<sup>7</sup> and does not show rise in value near  $1 \text{ kHz}$  as shown by them indicating space charge resonance.

The  $\epsilon$  values are observed to decrease with increase in calcium content from  $x = 0.1$  to  $0.5$  for the frequencies more than  $1 \text{ kHz}$ , however, an increase in these values is observed in the same frequency range from  $x = 0.0$  to  $0.1$ . The dielectric loss or dissipation factor is the amount of energy dissipated in rotation of atomic dipoles and it depends on the following factors: (a) frequency, (b) temperature and (c) nature of additives.<sup>18,19</sup> The frequency dependence of loss values is shown in Fig. 5. The  $x = 0.0, 0.2$  and  $0.3$  samples

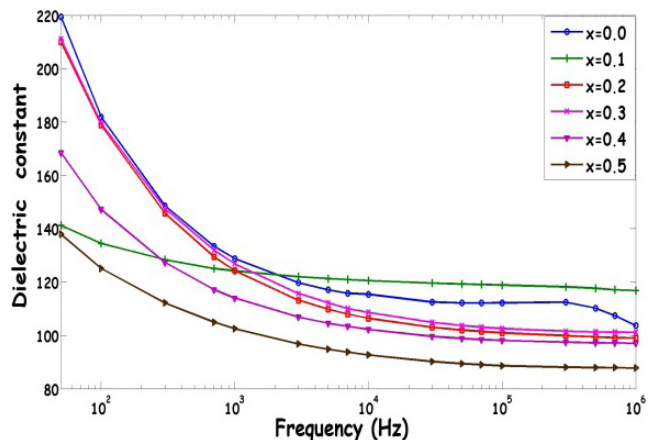


Fig. 4. Dielectric constant versus frequency behavior of calcium substituted  $\text{Sr}_{1-x}\text{Ca}_x\text{Bi}_2\text{Nb}_2\text{O}_9$  samples.

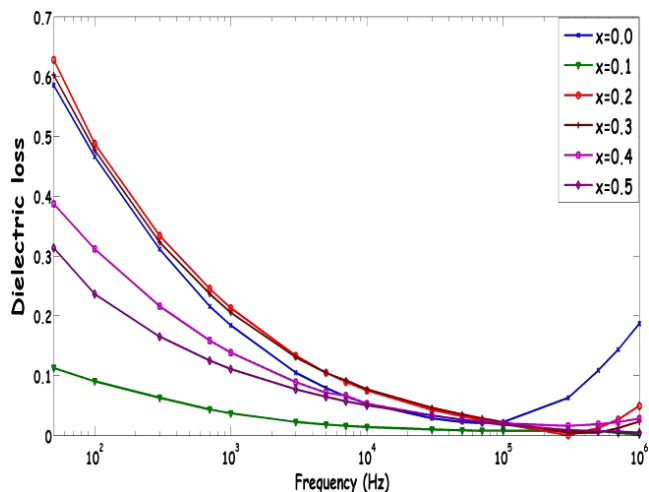


Fig. 5. Dielectric loss versus frequency behavior of  $\text{Sr}_{1-x}\text{Ca}_x\text{Bi}_2\text{Nb}_2\text{O}_9$  samples.

show higher dielectric loss whereas loss values for  $x = 0.1$ , 0.4 and 0.5 samples are low. All samples show a decrease in loss values up to a frequency of 100 kHz and there is an indication of slight increase at higher frequencies. The  $x = 0.1$  sample shows lowest loss in the frequency range and this was also observed by Forbess *et al.*<sup>7</sup> It is known that space charge contributes for leakage current, which is the source of dielectric loss.<sup>20</sup> Therefore, increase in dielectric loss for  $x = 0.0$ , 0.2 and 0.3 samples should be attributed to the presence of space charge and this interpretation is in conformity with the dielectric constant versus frequency observations.

The source of dielectric loss in the insulating ceramics is space charge relaxation. Additionally, domain wall motion under the external electric field may influence the dissipation factor. The doping of calcium is known to inhibit domain wall motion therefore greater energy should be consumed in rotating dipoles in the structure even at room temperature.<sup>21–23</sup> The loss in undoped SBN sample is mainly because of space charge content but in doped samples it is attributed to inhibited domain wall motion. The samples with  $x = 0.1–0.3$  are observed to support the argument, from Fig. 5, low space charge in  $x = 0.2$  and 0.3 samples as compared to undoped SBN can be seen. However, higher dielectric constant values up to 1 kHz in 0.2 and 0.3 samples against 0.1 sample indicate the presence of greater space charge cascading with dipoles to increase the capacitance. Therefore, high loss values are expected in these samples, which are observed too. The  $x = 0.4$  and 0.5 samples are observed to possess lesser space charge and thus low loss values as compared to 0.2 and 0.3 samples.

In Fig. 6,  $\epsilon$  versus temperature behavior of a few calcium introduced SBN ceramics is shown. These measurements are taken at frequency 100 kHz at which space charge and orientational polarizations are saturated off, only ionic and electronic contributions persist.<sup>17</sup> These ceramics are known

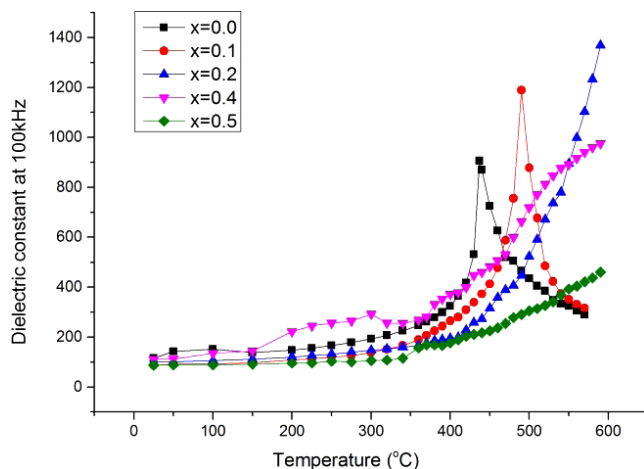


Fig. 6. Dielectric constant versus temperature behavior of  $\text{Sr}_{1-x}\text{Ca}_x\text{Bi}_2\text{Nb}_2\text{O}_9$  samples.

to have single-phase ferroelectric to paraelectric phase transitions at a temperature where dielectric constant is maximum, i.e., Curie temperature.<sup>18</sup> Single-phase transitions are observed in samples  $x = 0.0$  and 0.1 at temperatures 437°C and 490°C, respectively. The  $x = 0.2$  and higher doped samples do not show transition up to 600°C, up to which present measurements are taken. This shows a large increase in Curie temperature with increase in calcium content. The samples with  $x = 0.1$ , 0.2, 0.4 and 0.5 are shown here. In Fig. 6, if the slope of each curve is studied then an increase in Curie temperature with increase in calcium doping is expected. Also, an increase in dielectric constant value for almost all doped samples is expected based on similar reasons.

Dielectric loss versus temperature behavior of a few compositions ( $x = 0.0$ , 0.1, 0.2, 0.4 and 0.5) at 100 kHz is shown in Fig. 7. The samples show nearly equal loss values up to 370°C. The sample with  $x = 0.5$  shows an increase at

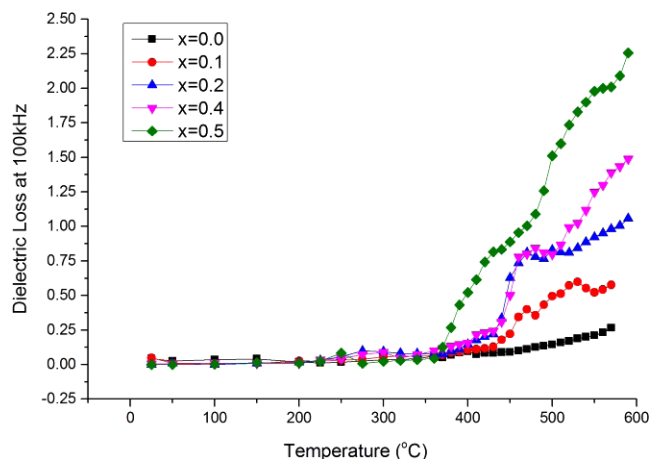


Fig. 7. Dielectric loss versus temperature behavior of a few  $\text{Sr}_{1-x}\text{Ca}_x\text{Bi}_2\text{Nb}_2\text{O}_9$  samples.

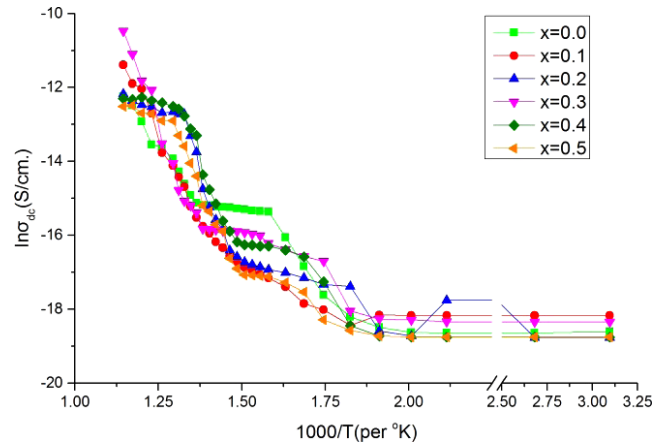


Fig. 8. dc conductivity versus temperature behavior of  $\text{Sr}_{1-x}\text{Ca}_x\text{-Bi}_2\text{Nb}_2\text{O}_9$  samples.

relatively low temperatures as compared to other doped and undoped sample. The behavior of loss values can be explained on the basis of intrinsic defect formation at such high temperatures and applied ac-field. The studied compositions are expected to have defects because of  $\text{Bi}_2\text{O}_3$  evaporation at high temperatures. Therefore, all samples should possess positive and negative charge carrier vacancies due to evaporation of bismuth and oxygen. The introduction of calcium onto the sites of strontium would ease the release of negative charge carriers (oxygen ions) at higher temperatures and therefore doped samples should show larger loss values; which is indeed observed.

Ionic dc conductivity ( $\sigma_{dc}$ ) values of all samples are plotted in Fig. 8 as Arrhenius plot. Intrinsic dc activation energy for all the samples is calculated using slope of these Arrhenius plots from  $400^\circ\text{C}$  to  $600^\circ\text{C}$ ; the observed values are shown in Table 3. The  $x = 0.5$  sample is found to possess maximum activation energy of 1.00 eV and  $x = 0.0$  sample minimum of 0.65 eV. At room temperature, conductivities are observed to decrease with increase in calcium content the reason for which could be tetragonal strain behavior of these samples. Room temperature dc conductivities of all samples are of the order of  $10^{-8}$  S/cm, which increase up to  $10^{-5}$  S/cm. at  $600^\circ\text{C}$ . Above  $450^\circ\text{C}$ , all doped samples show high conductivities compared to undoped one. Below  $450^\circ\text{C}$ ,

Table 3. Intrinsic dc activation energy and room temperature conductivity of samples.

Composition (x) in $\text{Sr}_{1-x}\text{Ca}_x\text{Bi}_2\text{Nb}_2\text{O}_9$	Intrinsic dc activation energy ( $E_a$ ) (in eV)	Room Temperature dc conductivity ( $\times 10^{-8}$ S/cm.)
0.0	0.65	0.83
0.1	0.81	0.79
0.2	0.96	0.75
0.3	0.90	0.72
0.4	0.98	0.71
0.5	1.00	0.67

multiple crossovers are seen alongwith low slope values on decreasing temperature particularly in phase transition temperature range ( $390^\circ\text{C} \leq T \leq 490^\circ\text{C}$ ). This might be because of increased kinetics as an outcome of expected negative temperature coefficient of resistance (NTCR) behavior to nullify unusual positive temperature coefficient of resistance (PTCR). The PTCR behavior is also known to exist in insulators with dominant anionic vacancy conduction (*n*-type conduction), which has been reported in  $\text{BaTiO}_3$ .<sup>24</sup> The temperature range  $390\text{--}470^\circ\text{C}$  is phase transition temperature range for undoped sample where it shows very low conductivity change. It indicates that possibly undoped SBN and samples with  $x = 0.1\text{--}0.5$  except  $x = 0.1$  contain large number of negative charge carriers, i.e., unsaturated oxygen ions because of higher bismuth loss due to the evaporation of volatile bismuth oxide. The loss of bismuth oxide is expected to increase with increase in calcium content due to lower calcium–oxygen bond strength and its increasing concentration at available atomic sites. Above  $450^\circ\text{C}$ , all doped samples are observed to possess high conductivities compared to undoped SBN sample. The influence of internal lattice strain is observed to affect conductivity in more direct fashion at room temperature only, greater is the internal strain, less conducting are the samples, therefore, observation from Fig. 2 for internal strain and that from third column of Table 3 are mutually supporting. The energy required for the formation of vacancy and its movement determining the conductivity of materials is called as activation energy.<sup>21</sup> This movement is always opposed by the internal lattice strain, which traps the free charge carriers and does not allow their migration. As internal lattice strain shows an increase with calcium doping, therefore, it is expected that the activation energy should increase correspondingly. This is exactly observed except marginally lower activation energy indicated by sample  $x = 0.3$ .

#### 4. Conclusion

Calcium substituted SBN ceramics are found to have increased dielectric constant and reduced dielectric loss values from room temperature to  $350^\circ\text{C}$ . Above  $350^\circ\text{C}$ , loss values increase according to increase in calcium content due to smoothed oxygen vacancy conduction. Although room temperature behavior of dielectric constant values is somewhat periodic with increase in calcium content, that is surprising. High dc activation energies of these samples can be utilized for setting higher operating temperature limit for capacitive and memory applications. The doping of calcium shows remarkable reduction in dielectric loss in SBN ceramics and improves their microstructure significantly. Internal lattice strain is observed to affect electrical response of these materials significantly apart from driving granular flow during processing to form better microstructure. The increase in calcium content in SBN is estimated to increase Curie

temperature of doped samples (for  $x = 0.2$  and above) above  $600^\circ\text{C}$  which is also in accordance with a few reports published earlier.

## References

- <sup>1</sup>H. Nagata, N. Chikushi and T. Takenaka, Ferroelectric properties of Bismuth layer structured compound  $\text{Sr}_x\text{Bi}_{4-x}\text{Ti}_{3-x}\text{Ta}_x\text{O}_{12}$ , *Jpn. J. Appl. Phys.* **38**(9B), 5497 (1999).
- <sup>2</sup>A. I. Kingon and S. K. Streiffer, Ferroelectric films and devices, *Curr. Opin. Solid State Mater. Sci.* **4**(1), 39 (1999).
- <sup>3</sup>C. A. P. Arauzo, J. D. Cuchlaro, L. D. Mcmillan, M. C. Scott and J. F. Scott, Fatigue-free ferroelectric capacitors with platinum electrodes, *Nature* **374**, 627 (1995).
- <sup>4</sup>K. Utsumi, Y. Shimada, T. Ikeda and H. Takamizawa, Monolithic multicomponents ceramic substrate, *Ferroelectrics* **68**(1), 157 (1986).
- <sup>5</sup>T. C. Chen, C. L. Thio and S. B. Desu, Impedance spectroscopy of  $\text{SrBi}_2\text{Ta}_2\text{O}_9$  and  $\text{SrBi}_2\text{Nb}_2\text{O}_9$  correlation with fatigue behavior, *J. Mater. Res.* **12**(10), 2628 (1997).
- <sup>6</sup>B. Aurivillius, Mixed bismuth oxides with layer lattices: The structure type of  $\text{CaNb}_2\text{Bi}_2\text{O}_9$ , *Arkiv Kemi* **1**, 463 (1949).
- <sup>7</sup>M. J. Forbess, S. Seraji, Y. Wu, C. P. Nguyen and G. Z. Cao, Dielectric properties of layered perovskite  $\text{Sr}_{1-x}\text{A}_x\text{Bi}_2\text{Nb}_2\text{O}_9$  ferroelectrics ( $A = \text{La}, \text{Ca}$  and  $x = 0, 0.1$ ), *Appl. Phys. Lett.* **76**(20), 2934 (2000).
- <sup>8</sup>E. W. Nuffield, *X-ray Diffraction Methods* (John Wiley & Sons Inc., NY, 1966).
- <sup>9</sup>A. Onodera, T. Kubo, K. Yoshio, S. Kojima, H. Yamashita and T. Takama, Crystal structure of high temperature paraelectric phase in Bi-layered perovskite  $\text{Sr}_{0.85}\text{Bi}_{2.1}\text{Ta}_2\text{O}_9$ , *Jpn. J. Appl. Phys.* **39**(9B), 5711 (2000).
- <sup>10</sup>Y. Wu, M. J. Forbess, S. Seraji, S. J. Limmer, T. P. Chou, C. Nguyen and G. Z. Cao, Doping effect in layer structured  $\text{SrBi}_2\text{Nb}_2\text{O}_9$  ferroelectrics, *J. Appl. Phys.* **90**(10), 5296 (2001).
- <sup>11</sup>M. P. Moret, R. Zallen, R. E. Newnham, P. C. Joshi and S. B. Deshu, Infrared activity in the Aurivillius layered ferroelectric  $\text{SrBi}_2\text{Ta}_2\text{O}_9$ , *Phys. Rev. B* **57**(10(A)), 5715 (1998).
- <sup>12</sup>D. Y. Suarez, Ian M. Reaney and W. E. Lee, Relation between tolerance factor and  $T_c$  in Aurivillius compounds, *J. Mater. Res.* **16**(11), 3139 (2001).
- <sup>13</sup>Y. Shimakawa, Y. Kubo, Y. Nakagawa, S. Goto, T. Kamiyama, H. Asano and F. Izumi, Crystal structure and ferroelectric properties of  $\text{ABi}_2\text{Ta}_2\text{O}_9$  ( $A = \text{Ca}, \text{Sr}$  and  $\text{Ba}$ ), *Phys. Rev. B* **61**(10), 6559 (2000).
- <sup>14</sup>R. D. Shannon and C. T. Prewitt, Effective ionic radii in oxides and fluorides, *Acta Crystallogr.* **B25**, 925 (1969).
- <sup>15</sup>K. Shibata, K. Shoji and K. Sakata,  $\text{Sr}_{1-x}\text{Ca}_x\text{Bi}_2\text{Ta}_2\text{O}_9$  piezoelectric ceramics with high mechanical quality factor, *Jpn. J. Appl. Phys.* **40**(9B), 5719 (2001).
- <sup>16</sup>R. R. Das, P. Bhattacharya, W. Perez, R. S. Katiyar and S. B. Deshu, Ferroelectric properties of laser-ablated  $\text{Sr}_{1-x}\text{A}_x\text{Bi}_2\text{Ta}_2\text{O}_9$  thin films, *Appl. Phys. Lett.* **80**(4), 637 (2002).
- <sup>17</sup>R. C. Buchanan, *Principles of Electronic Ceramics* (Marcel Dekker, New York, 1991), pp. 38–39.
- <sup>18</sup>E. C. Subbarao, Ferroelectricity in mixed Bismuth oxides with layer type structure, *J. Chem. Phys.* **34**, 695 (1961).
- <sup>19</sup>L. L. Hench and D. B. Dove, *Physics of Electronic Ceramics, Part A* (Marcel Dekker, New York, 1971), p. 479.
- <sup>20</sup>B. Tareev, *Physics of Dielectric Materials* (Mir Publishers, Moscow, 1971), p. 148.
- <sup>21</sup>I. S. Zheludev, *Physics of Crystalline Dielectrics*, Vol. 2 (Plenum Press, NY, 1971).
- <sup>22</sup>A. Ando, M. Kimura and Y. Sakabe, Piezoelectric properties of Ba and Ca doped  $\text{SrBi}_2\text{Nb}_2\text{O}_9$  based ceramic materials, *Jpn. J. Appl. Phys.* **42**, Part 1 (2A), 520 (2003).
- <sup>23</sup>S. E. Park, J. A. Cho, T. K. Song, M. H. Kim, S. S. Kim and H. S. Lee, Ionic doping effects in  $\text{SrBi}_2\text{Nb}_2\text{O}_9$  ferroelectric ceramics, *J. Electroceram.* **13**, 51 (2004).
- <sup>24</sup>C. Ang, Z. Yu and L. E. Cross, Oxygen-vacancy related low-frequency dielectric relaxation and electrical conduction in  $\text{Bi:SrTiO}_3$ , *Phys. Rev. B* **62**(1), 228 (2000).